Design of Unity Power Factor Controller for Three-phase Induction Motor Drive Fed from Single Phase Supply

Rachana Garg[1], Priya Mahajan[1], Parmod Kumar[2], and Rohit Goyal[1]
[1]Delhi Technological University, New Delhi 110042, India
[2]Maharaja Agrasen Institute of Technology, New Delhi 110085, India
Email: {rachana16100, pramodk2003}@yahoo.co.in, {priyamahajan.eed, rohitelect.goyal} @gmail.com

***Abstract*— This paper carves out the design of unity power factor controller for three phase variable speed induction motor drive. SPWM technique is used to improve the power factor of the system to unity and hysteresis controller is used for speed control of the drive. These control techniques lead to a unity power factor seen by the ac supply and minimize the power loss, audible noise, and motor torque ripple. A three level converter-inverter system employing advanced insulated gate bipolar transistors (IGBTs) is used.**

***Index Terms*—Ac-dc-ac converter; vector controlled induction motor drive; unity power factor control, Hysteresis controller**

I. Introduction

Induction motor is widely used in industry and agricultural sector due to the fact that it is relatively cheap, rugged and maintenance free. It needs reactive power for operation and working. Thus, a large reactive power is required to be supplied and transmitted which reduces the power factor of the system and hence the transmission lines capacity. It is therefore desirable to improve the power factor of supply side for induction motor drive. This can be achieved using unity power factor (upf) controller with sinusoidal pulse width modulation (SPWM) technique. In the present work, the authors have simulated the IGBT based power converter, connected to three phase induction motor drive. Hysteresis controller is used for variable speed control.

A lot of research has been going on to improve the performance and efficiency of the induction drive system. K. Thiyagarajah, V. T. Ranganathan described an inverter/converter system operating from a single - phase supply using IGBT [1]. Adrian David Cheok, Shoichi Kawamoto, Takeo Matsumoto, and Hideo Obi described new developments in the design of high-speed electric trains with particular reference to the induction motor drive system [2]. Prasad N. Enjeti, and Ashek Rahman have proposed the new single-phase to three-phase converter for low-cost ac motor drive [3]. The different control strategy of induction motor drive system has been presented and discussed by various researchers [4]-[6].

Manuscript received August 1, 2013; revised November 5, 2013.

II. Problem Formulation

The induction motor drive comprises of (i) ac to dc converter, (ii) dc to ac inverter, and (iii) dc link capacitor between the converter and inverter. Fig. 1 shows the proposed configuration for unity power factor control towards power supply to induction motor drive. The front-end for the system used here is a full-bridge IGBT PWM converter with an ac reactor [7]. In order to maintain the supply current at unity power factor, unity power factor controller with SPWM technique is designed.

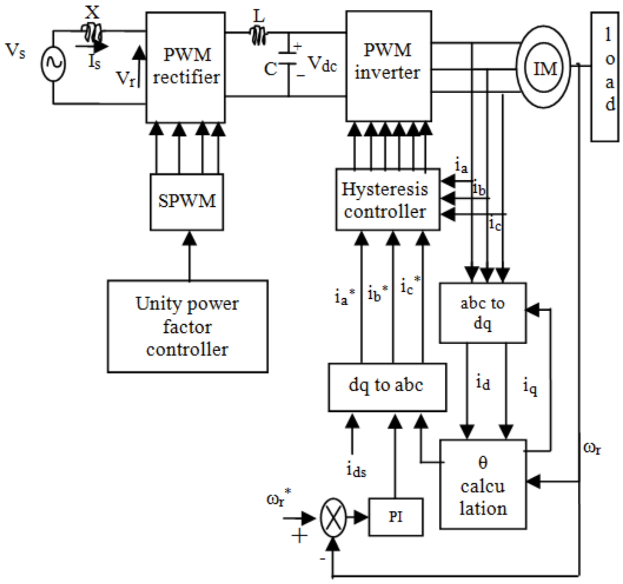

Figure 1. Block diagram of supply side unity power factor control of induction motor drive

On the machine side, a high switching frequency three phase PWM inverter using IGBT is used. This converter is controlled by hysteresis controller for variable speed drive. The entire system is fed from single-phase mains supply.

III. Power Factor Control Algorithm

To achieve unity power factor on supply side, input voltage to converter, V_r, is controlled with current and

doi: 10.12720/joace.2.3.221-227

voltage feedback to control the phase difference between the ac supply voltage and current. In the unity power factor case, the converter voltage amplitude is given by (1) [8]

$$V_r = \sqrt{V_s^2 + (I_s X_s)^2} \quad (1)$$

If the converter voltage can be controlled to the above value then unity power factor will be maintained. In the developed upf controller, a control system is used to maintain unity power factor by controlling the switching of converter. The upf controller maintains a constant dc output voltage, in order that a steady dc link voltage is fed to the inverter. The block diagram of unity power factor controller algorithm is shown in Fig. 2.

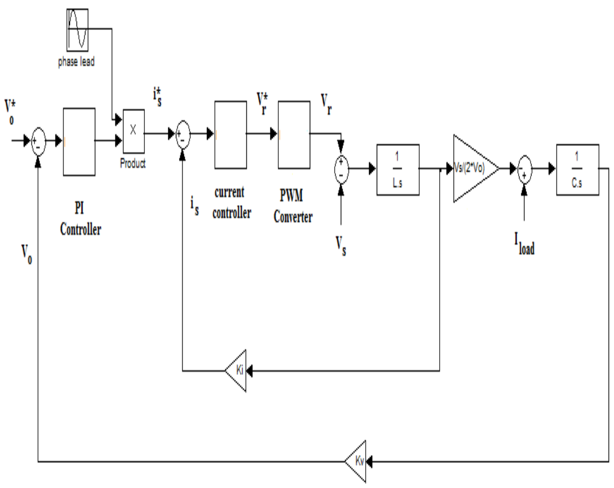

Figure 2. Block Diagram of Unity Power Factor Control Algorithm

IV. DYNAMIC MODEL OF INDUCTION MOTOR

The three phase squirrel cage induction motor in synchronous rotating reference frame can be represented as in Fig. 3[9].

Voltage and flux equations for the motor are given by (2)-(9)[9].

$$V_{qs} = R_s * i_{qs} + \frac{d\varphi_{qs}}{dt} + \omega_e \varphi_{ds} \quad (2)$$

$$V_{ds} = R_s * i_{ds} + \frac{d\varphi_{ds}}{dt} - \omega_e \varphi_{qs} \quad (3)$$

$$V_{qr} = R_r * i_{qr} + \frac{d\varphi_{qr}}{dt} + (\omega_e - \omega_r)\varphi_{dr} \quad (4)$$

$$V_{dr} = R_r * i_{dr} + \frac{d\varphi_{dr}}{dt} - (\omega_e - \omega_r)\varphi_{qr} \quad (5)$$

$$\varphi_{qs} = L_{ls} * i_{qs} + (i_{qs} + i_{qr}) L_m \quad (6)$$

$$\varphi_{qr} = L_{lr} * i_{qr} + (i_{qs} + i_{qr}) L_m \quad (7)$$

$$\varphi_{ds} = L_{ls} * i_{ds} + (i_{ds} + i_{dr}) L_m \quad (8)$$

$$\varphi_{dr} = L_{lr} * i_{dr} + (i_{ds} + i_{dr}) L_m \quad (9)$$

where V_{qs} & V_{ds} are the applied voltages to the stator; i_{ds}, i_{qs}, i_{dr}, & i_{qr} are the corresponding d & q axis currents; φ_{qs}, φ_{qr} & φ_{ds}, φ_{dr} are the rotor & stator flux component; R_s, R_r are the stator & rotor resistances; L_{ls} & L_{lr} denotes the stator & rotor inductances, L_m is the mutual inductance.

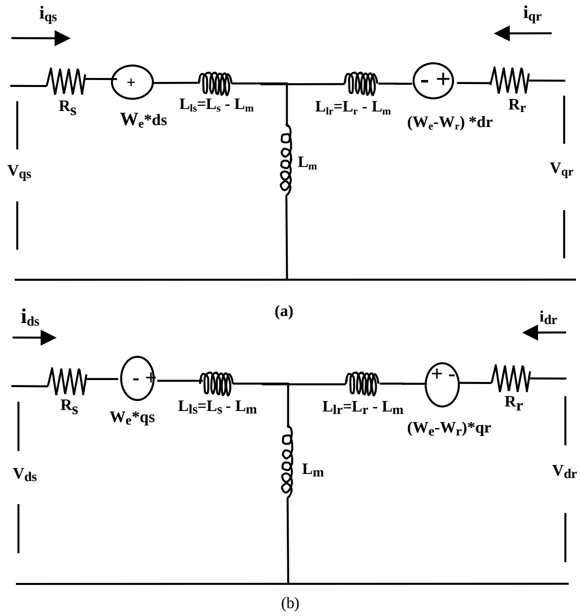

Figure 3. Equivalent circuit of Induction motor in synchronous rotating reference frame, a) q-axis circuit b) d-axis circuit

The electromagnetic torque equation is given by (10)

$$T_e = \frac{3 * P * L_m}{2 * 2 * L_r} * \left(\varphi_{dr} i_{qs} - \varphi_{qr} i_{ds}\right) \quad (10)$$

where *P* denotes the pole number of the motor

In case of vector control the *q*-component of the rotor field φ_{qr} would be zero. Then the electromagnetic torque is controlled only by *q*-axis stator current & (10) is reduced to (11)

$$T_e = \frac{3 * P * L_m}{2 * 2 * L_r} * \left(\varphi_{dr} i_{qs}\right) \quad (11)$$

V. VECTOR CONTROL METHODOLOGY

There are large number of ways for speed control of induction motor among which vector or field oriented control is the most widely accepted methods now a day's[9]-[15]. In the present studies indirect vector control method is employed. Here, the unit vector is generated in an indirect manner using the measured speed ω_r and slip speed ω_{sl}. The following dynamic equations take into consideration to implement indirect vector control strategy. Equation 12 shows the rotor flux position.

$$\theta_e = \int \omega_e dt = \int (\omega_r + \omega_{sl}) dt = \theta_r + \theta_{sl} \quad (12)$$

The stator current i_a, i_b, i_c in the 3-phase coordinate is changed to 2-phase AC current in the static coordinate with 3/2 equivalent transformation. Then through synchronous rotating coordinate transformation, the 2-phase AC current will be equivalent as dc current i_d and i_q in the synchronous rotating coordinate. The *abc-dq* transformation is an essential part of this scheme. The direct–quadrature–zero (*dq*o) transformation or zero–

direct–quadrature (o*dq*) transformation is a mathematical transformation used to simplify the analysis of three-phase circuits. The transformation of abc-dq involves the decoupling of variables with time-varying coefficients and refers all variables to a common *reference* frame. This transformation reduces the three line currents to two dc quantities in dq reference frame. The two dc quantities are orthogonal to each other. This allows the control of the two quantities independently. The three-phase transformation into two-phase is carried out through *abc-dq* transformation by using various methods like Stanley's transformation, Park's transformation etc. Park's transformation applied to three-phase currents is shown by (13)

$$I_{dqo} = TI_{abc} = \frac{2}{3}\begin{bmatrix} \cos\theta & \cos\left(\theta - \frac{2\pi}{3}\right) & \cos\left(\theta + \frac{2\pi}{3}\right) \\ -\sin\theta & -\sin\left(\theta - \frac{2\pi}{3}\right) & -\sin\left(\theta + \frac{2\pi}{3}\right) \\ 0.5 & 0.5 & 0.5 \end{bmatrix}\begin{bmatrix} I_a \\ I_b \\ I_c \end{bmatrix} \quad (13)$$

The inverse transform is shown by (14)

$$I_{abc} = T^{-1}I_{dqo} = \begin{bmatrix} \cos\theta & -\sin\theta & 1 \\ \cos\left(\theta - \frac{2\pi}{3}\right) & -\sin\left(\theta - \frac{2\pi}{3}\right) & 1 \\ \cos\left(\theta + \frac{2\pi}{3}\right) & -\sin\left(\theta + \frac{2\pi}{3}\right) & 1 \end{bmatrix}\begin{bmatrix} I_d \\ I_q \\ I_o \end{bmatrix} \quad (14)$$

VI. Hysteresis Current Control Algorithm:

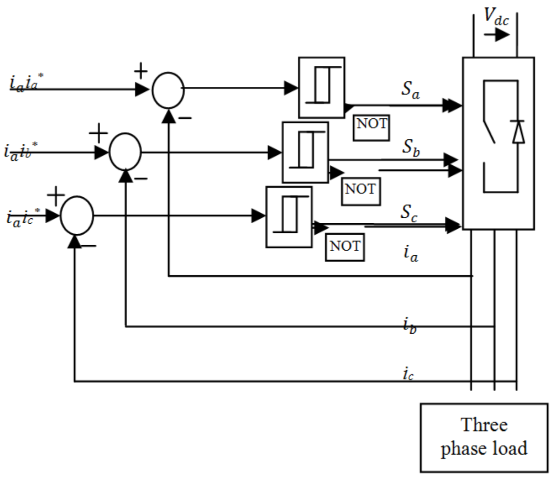

Figure 4. Block diagram of hysteresis current control

Fig. 4 shows the block diagram for hysteresis current control scheme for induction motor drive. In this circuit three phase load i.e induction motor in our case is connected to the PWM voltage source inverter. Hysteresis current algorithm is used to control the speed of induction motor. The load currents i_a, i_b and i_c are compared with the reference currents i_a*, i_b* and i_c* and error signals are passed through hysteresis band to generate the firing pulses, which are operated to produce output voltage in manner to reduce the current error. The purpose of the current controller is to control the load current by forcing it to follow a reference one. It is achieved by the switching action of the inverter to keep the current within the hysteresis band. The load currents are sensed & compared with respective command currents by three independent hysteresis comparators having a hysteresis band '*h*'. The output signals of the comparators are used to activate the inverter power switches. The inverter current vector is given by (15)

$$i = \frac{2}{3}[i_a + \alpha i_b + \alpha^2 i_c] \quad (15)$$

where α is complex number operator

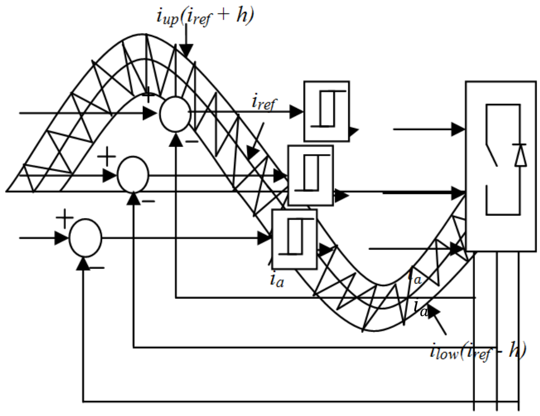

Figure 5 Fixed band shape of hysteresis controller

In this scheme, the hysteresis bands are fixed throughout the fundamental period. Fig. (5) Shows the fixed band shape of hysteresis controller. The algorithm for one phase of this scheme is given by (16)-(18)

$$i_{ref} = i_{max} sin\omega t \quad (16)$$

Upper band limit of current

$$i_{up} = i_{ref} + h \quad (17)$$

Lower band limit of current

$$i_{low} = i_{ref} - h \quad (18)$$

where, *h* = Hysteresis band limit

If $\quad i_a > i_{up}, \quad V_{ao} = -V_{dc}/2$

If $\quad i_a < i_{low}, \quad V_{ao} = +V_{dc}/2$

VII. Simulation Results and Discussion

The simulation has been carried on the 3-phase, 5hp (3.73KW), 1750rpm (183.33rad/sec), 50Hz squirrel cage induction motor with following parameters:

Stationary reference frame
Y- Connected
R_s (stator resistance) = 1.115Ω
R_r (rotor resistance) = 1.083Ω
L_s (stator inductance) = 0.005974H
L_r (rotor inductance) = 0.005974H
L_m (magnetizing inductance) = 0.2037H
J (moment of inertia) = 0.02Kg m^2
P (number of poles) = 4

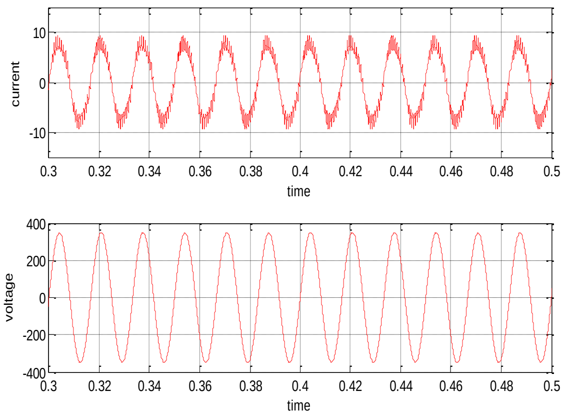

(a)

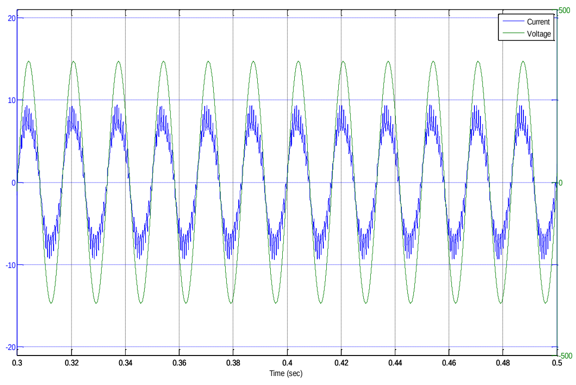

(b)

Figure 6. (a)and (b) Simulink plot showing supply side unity power factor control on "no load" at 60 rad/sec

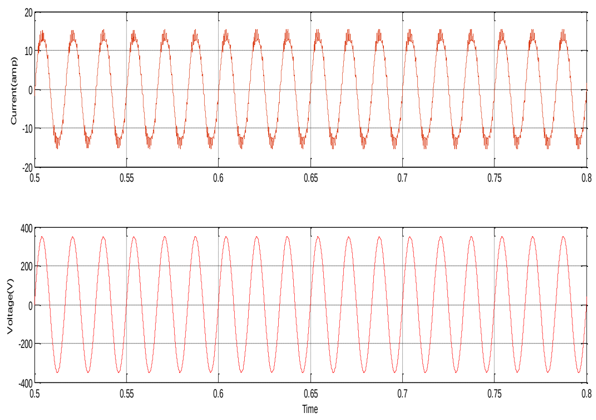

(a)

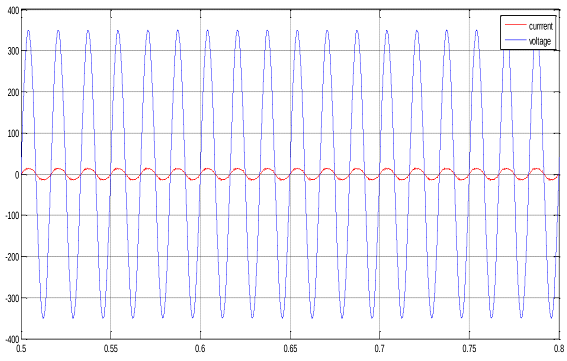

(b)

Figure 7. (a)and (b) Simulink plot showing supply side unity power factor control on "full load" at 60 rad/sec

Fig. 6-Fig. 9 shows the supply side unity power factor control on different speed and different load.

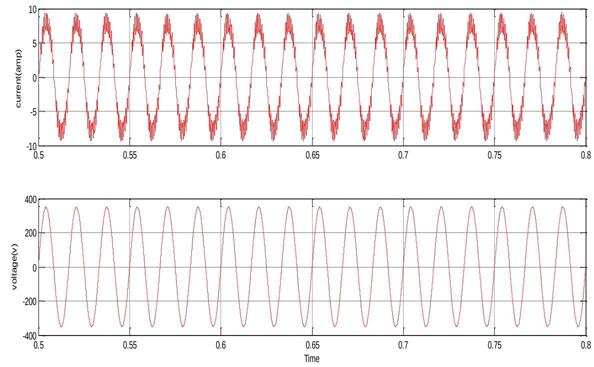

(a)

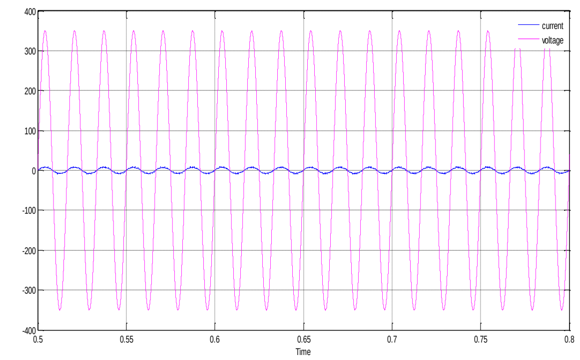

(b)

Figure 8. (a)and (b) Simulink plot showing supply side unity power factor control on "no load" at 150 rad/sec

Fig. 10-Fig. 13 shows the voltage (line-line), three phase stator current, speed and electromagnetic torque on different load and different speed with respect to time.

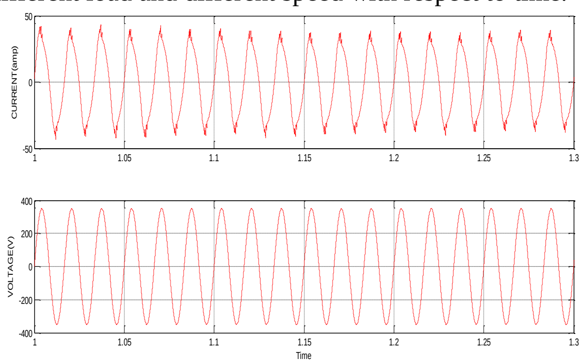

(a)

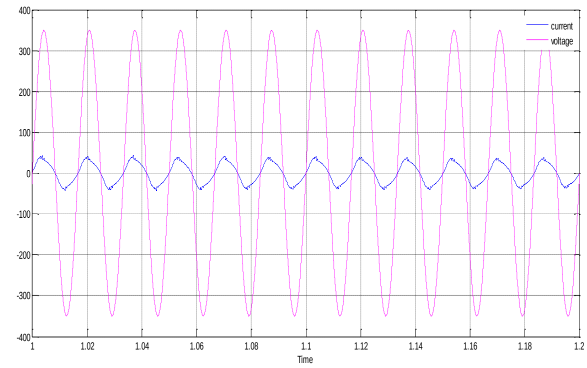

(b)

Figure 9. (a)and (b) Simulink plot showing supply side unity power factor control on "full load" at 140 rad/sec

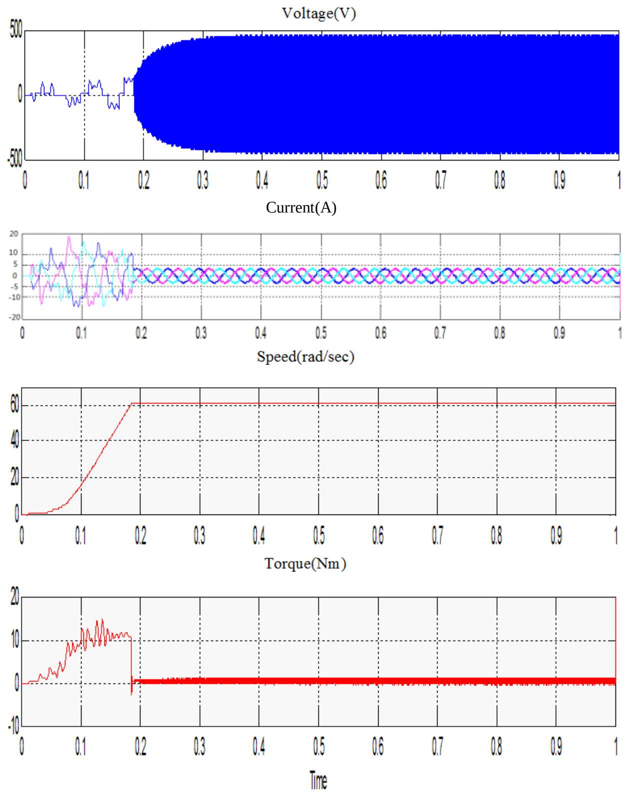

Figure 10. Simulink plot showing voltage (line-line), three phase stator current, speed and electromagnetic torque on “no load” at 60rad/sec speed with respect to time

Fig. 6 shows the simulink result of supply side unity power factor control of 5hp induction motor working on “no load” at 60 rad/sec. It has been observed that at no load supply side current is 8.1A peak current but at improved power factor of approximately unity. The current contains nominal harmonics.

Fig. 7 shows the simulink result of supply side unity power factor control of 5hp induction motor working on “full load” at 60 rad/sec, it has been observed that at full load supply side current is 12.1A peak current but at improved power factor of approximately unity. The current contains nominal harmonics.

Fig. 8 shows the simulink result of supply side unity power factor control of the 5hp induction motor working on “no load” at 150 rad/sec. It has been observed that at no load supply side current 8.1 A peak current but at improved power factor of approximately unity. The current contains nominal harmonics.

Fig. 9 shows the simulink result of supply side unity power factor control of 5hp induction motor working on “full load” at 140 rad/sec, it has been observed that at full load supply side current is 30A peak current but at improved power factor of approximately unity, the current contains nominal harmonics.

Fig. 10 shows voltage (line-line), three phase stator current, speed and electromagnetic torque of 5hp induction motor on “no load” at 60 rad/sec. The no load current per phase is 3.2A peak. The currents show a hysteresis band of variation. The three phase currents are perfectly sinusoidal, 120^{o} apart from each other. At the time of starting the maximum current drawn by the induction motor is as high as 18A peak. Initially current frequency is low due to this at the time of starting torque is more.

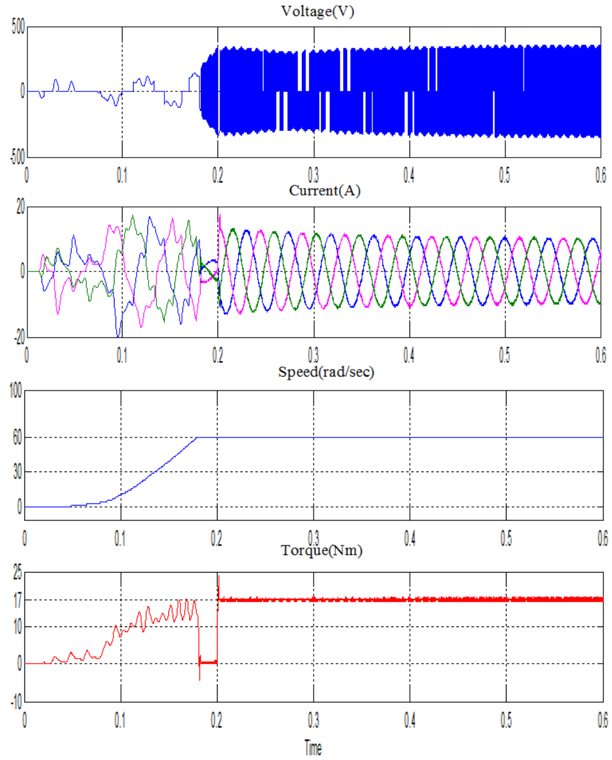

Figure 11. Simulink plot showing voltage (line-line), three phase stator current, speed and electromagnetic torque on “full load” at 60rad/sec speed with respect to time

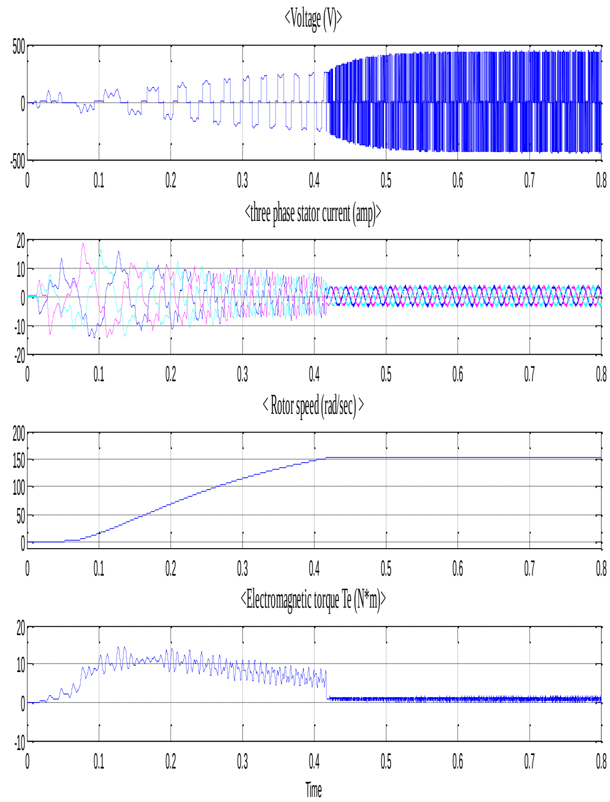

Figure 12. Simulink plot showing voltage (line-line), three phase stator current, speed and electromagnetic torque on “no load” at 150rad/sec speed with respect to time

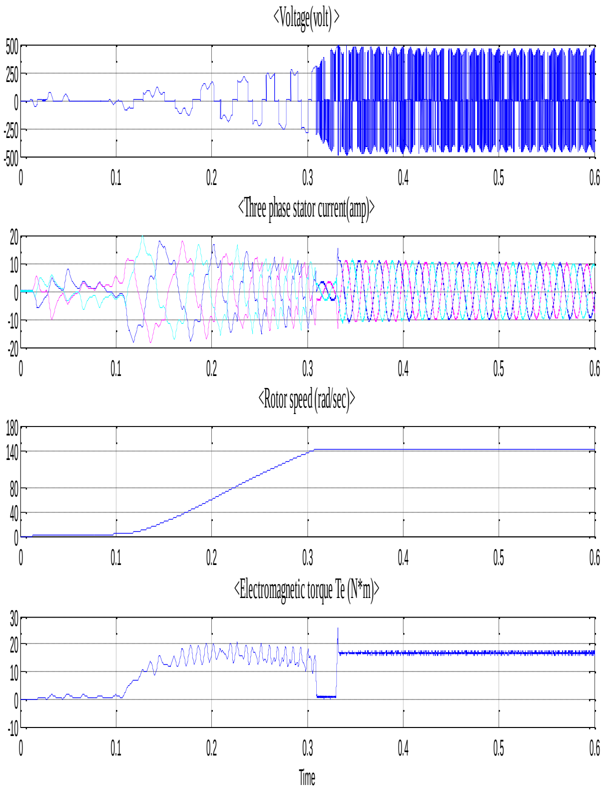

Figure. 13. Simulink plot showing voltage (line-line), three phase stator current, speed and electromagnetic torque on "full load" at 140rad/sec speed with respect to time

Fig. 11 shows voltage (line-line), three phase stator current, speed and electromagnetic torque of 5hp induction motor on "full load" at 60 rad/sec. The full load current is 9.4A peak. The current shows a hysteresis band of variation. The three phase currents are perfectly sinusoidal, 120^o apart from each other. At the time of starting the maximum current drawn by the induction motor is as high as 18A peak. Initially current frequency is low due to this at the time of starting torque is more.

Fig. 12 shows voltage (line-line), three phase stator current, speed and electromagnetic torque of 5hp induction motor on "no load" at 150 rad/sec. The no load current is 3.2 A peak. The currents show a hysteresis band of variation. The three phase currents are perfectly sinusoidal, 120^o apart from each other. At the time of starting the maximum current drawn by the induction motor is as high as 18A peak. Initially current frequency is low. Due to this, at the time of starting, torque is more.

Fig. 13 shows voltage (line-line), three phase stator current, speed and electromagnetic torque of 5hp induction motor on "full load" at 140 rad/sec. The full load current per phase is 9.4 A peak. The current shows a hysteresis band of variation. The three phase currents are perfectly sinusoidal, 120^o apart from each other. At the time of starting the maximum current drawn by the induction motor is as high as 18A peak.

VIII. Conclusions

Simulation studies have been carried out using MATLAB 7.7.0 (R2008b) to control the speed of induction motor and improving the power factor of supply side to unity. The speed is controlled using hysteresis current controller, which controls the frequency of stator current. The results are taken for different values of speed under both no load and full load condition. It has been observed that the power factor can be controlled to unity at all speeds. The above studies are useful in improving the performance and efficiency of the supply system by decreasing the reactive power requirement of the system.

References

[1] K. Thiyagarajah, V. T. Ranganathan, and B. S. R. Iyengar, "A high switching frequency IGBT PWM rectified inverter system for ac motor drives operating from single phase supply," *IEEE Trans. on Power Electronics*, vol. 6, no. 4, October 1991.

[2] A. D. Cheok, S. Kawamoto, T. Matsumoto, and H. Obi, "High power AC/DC converter and DC/AC inverter for high speed train applications," in Proc. *TENCON*, 2000, pp. 423-428.

[3] P. Enjeti, and A. Rahman, "A new single phase to three phase converter with active input current shaping for low cost AC motor drives," *IEEE Trans. Industrial Applications*, vol. 29, no. 2, pp. 806–813, July 1993.

[4] J. Itoh, and K. Fujita, "Novel unity power factor circuits using zero-vector control for single-phase input systems," *IEEE Trans. Power Electronics.*, vol. 15, no. 1, pp. 36–43, Jan. 2000.

[5] B. K. Lee, B. Fahimi, and M. Ehsani, "Overview of reduced parts converter topologies for AC motor drives," in *Proc. IEEE PESC*, 2001, pp. 2019–2024.

[6] C. B. Jacobina, M. B. de R. Correa, A. M. N. Lima, and E. R. C. da Silva, "AC motor drive systems with a reduced switch count converter," *IEEE Trans. Industrial Appications*, vol. 39, no. 5, pp. 1333–1342, Sep./Oct. 2003.

[7] J. R. Rodrıguez, J. W. Dixon, J. R. Espinoza, J. Pontt, and P. Lezana, "PWM regenerative rectifiers: State of the art," *IEEE Trans. Industrial Electronics*, vol. 52, no. 1, pp. 5–22, Feb 2005.

[8] C. W. Lander, *Power Electronics*, McGraw-Hill Book Company.

[9] B. K. Bose, *Modern Power Electronics & AC Drives*, Prentice Hall.

[10] R. G. W. Leonhard, and C. J. Nordby, "Field-Oriented control of a standard ac motor using microprocessors," *IEEE Trans. on Industrial Applications*, vol. IA-16, no. 2, pp 186-192, March 1980.

[11] T. Matsuo, and T. A. Lipo, "A rotor parameter identification scheme for vector-controlled induction motor drives," *IEEE Trans. Industrial Appications*, vol. IA-21, no. 4, pp 624-632, May 1985.

[12] M. Koyama, M. Yano, I. Kamiyama, And S. Yano, "Microprocessor-based vector control system for induction motor drives with rotor time constant identification function," *IEEE Trans. on Industrial Applications*, vol. IA-22, no. 3, pp 453-459, May 1986.

[13] I. Takahashi, and T. Noguchi, "A new quick-response and high-efficiency control strategy of an induction motor," *IEEE Trans. on Industrial Applications*, vol. IA-22, no. 5, pp 820-827, Sept. 1986.

[14] T. Murata, T. Tsuchiya, and I. Takeda, "Vector control for induction machine on the application of optimal control theory," *IEEE Trans. on Industrial Electronics*, vol. 31, no. 4, August 1990.

[15] N. Mohan, T. M. Undeland, and W. P. Robins, *Power Electronics: Converters Applications and Design*, New York: Wiley, 1989.

Rachana Garg received the B.E. and M.E. degree in 1986 and 1989 from NIT, Bhopal respectively. She has obtained her Ph.D in Electrical Engg. from Delhi University in 2009.
Presently, she is working as Associate Prof. in Delhi Technological University, Delhi. Her area of interest is modeling of transmission lines, power system operation and control.

Priya Mahajan received the B.E. and M.E. degree in 1996 and 1998 from Thapar Institute of Engg. & Tech., Patiala and Punjab Engg. College, Chandigarh respectively. Presently she is pursuing the Ph.D degree in electrical engineering from Delhi University, Delhi.

She is working as Assistant Prof. in Delhi Technological University, Delhi since last 13 years. Her area of interest includes power system and railway traction system.

Parmod Kumar received the B.E., M.E., and Ph.D. degrees in 1972, 1975, and 1982, respectively.
After post-graduation in measurement and instrumentation, he joined M.P. Electricity Board, M.P., India, as an Assistant Engineer and commissioned telemetry and SCADA instruments at substations, power stations, and the central control room. In 1983, he joined the Central Electricity Authority as a Dynamic System Engineer and designed and configured the load dispatch centers for electric utilities. Subsequently, he served on various capacities to Indian Railway Construction Company, ERCON, ESPL, ESTC, and then entered academic life in 1991. His area of interest is smart and intelligent system design, operation, and control.

Rohit Goyal received B.E. degree in 2010 from M.B.M engineering college, Jodhpur and he is a M.tech student at Delhi Technological University, Delhi. He has completed the course work in M.tech and final result is awaited.
Presently, he is working as Assistant Prof. in Dehradun Institute Technology University, Dehradun. His areas of interest are railway traction system and control.